

## Research Article

# Epoxy-Glass Microballoon Syntactic Foams: Rheological Optimization of the Processing Window

A. V. Ullas <sup>1,2</sup>, Devendra Kumar,<sup>2</sup> and Prasun Kumar Roy <sup>1</sup>

<sup>1</sup>Centre for Fire, Explosive and Environment Safety, DRDO, Timarpur, Delhi 110054, India

<sup>2</sup>Department of Applied Chemistry and Polymer Technology, Delhi Technological University, Delhi 110042, India

Correspondence should be addressed to Prasun Kumar Roy; [pkroy@cfees.drdo.in](mailto:pkroy@cfees.drdo.in)

Received 30 October 2018; Accepted 24 February 2019; Published 1 April 2019

Academic Editor: Minna Hakkarainen

Copyright © 2019 A. V. Ullas et al. This is an open access article distributed under the Creative Commons Attribution License, which permits unrestricted use, distribution, and reproduction in any medium, provided the original work is properly cited.

In this paper, we discuss the chemorheology of epoxy based syntactic foams containing glass microballoons of varying density, with an aim of establishing the effect of microballoon loading on its processability. The primary objective is to determine the maximum microballoon loading that disperses uniformly in the resin without the aid of any diluent. The viscosity and dynamic mechanical properties of epoxy formulations containing varying amounts of glass microballoons were established by parallel plate rheometry. Our studies reveal that solventless processing of formulations with microballoon loading > 60% poses practical difficulties due to prohibitively high viscosities, although a packing efficiency of 74% is theoretically allowed in the case of hexagonal close packing. The presence of microballoons does not alter the curing mechanism. The mechanical properties of syntactic foams were inversely proportional to the loading and type of glass microballoons.

## 1. Introduction

Syntactic foams are lightweight composite materials prepared by incorporating hollow microballoons of glass [1], polymer [2, 3], or metal [4] in a suitable matrix. The inclusion of these hollow counterparts allows for significant weight savings, which is crucial for certain applications, especially marine [5, 6], aerospace [7, 8], and blast mitigation [9]. Polymeric syntactic foams refer to a subclass of cellular material, where hollow fillers are dispersed within a mechanically robust polymeric matrix. Apart from the nature of the matrix, concentration and type of microballoon are critical parameters, which decide its final properties [10]. Amongst hollow fillers, glass microballoons (HGM) are most extensively used [11–14], due to their low coefficient of thermal expansion and chemical inertness. Amongst all polymeric matrices, epoxy has been extensively studied [15–20], in view of its excellent mechanical properties and low shrinkage [21, 22].

The density of syntactic foam decreases with increasing concentration of purposely placed voids and for maximal weight savings, high loadings of the microballoon are desirable. The density of the syntactic foam can further be tuned

by astute choice of microballoons, which are available in a variety of sizes and grades. Hexagonal close packing of rigid spheres is expected for microballoon loading to 74% v/v [23]. However, it is very unlikely to achieve hexagonal close packing under conventional conditions employed for processing. Interestingly, assuming random packing, the upper limit of microballoon loading is restricted to ~ 64% v/v [24–26]. It is perhaps for this reason that very few studies deal with syntactic foams with very high microballoon loading ( $\phi > 60\%$ ) [8, 27–30].

Syntactic foams are conventionally processed using molding, casting, extrusion, rotational molding, or buoyancy methods, with the choice of technique depending upon the microballoon loading and the type of product being manufactured [31–33]. Processing using conventional techniques mandates fluidity of formulation for subsequent casting into molds. Increasing the microballoon loading beyond a critical value may render its processing impracticable by stir-casting techniques, which is perhaps most common. It is very important to establish the relationship of viscosity with curing time to ascertain optimal conditions required for processing. Surprisingly, rheological studies on syntactic

TABLE 1: Characteristics of hollow glass microballoons [2].

HGM	Density ( $\text{kgm}^{-3}$ )	Wall thickness ( $\mu\text{m}$ )	Radius ratio	Microballoon size (mean diameter) ( $\mu\text{m}$ )	Isostatic crush strength (MPa)	Thermal conductivity ( $\text{Wm}^{-1}\text{K}^{-1}$ ) at 21°C
K15	150	0.70	0.9839	43.6	2	0.055
K46	460	1.29	0.9356	40	41	0.153

foam formulations are rather scarce, with most of the studies dealing with the thermoplastic matrix [34–36]. In general, processing of compositions containing high microballoon loading is possible through molding [31], and casting mandates the use of solvent [14]. Unfortunately, there are issues associated with the subsequent solvent removal step, which in turn leads to void formation and a concomitant decrease in mechanical properties and increased production costs.

Chemorheology of curing thermosets has been widely studied and extensive reviews are available [37, 38]. Surprisingly, the rheological behavior of HGM-epoxy formulations has not been reported, which instigated us to undertake this work. Here, in this work, we attempt to establish the role played by HGM towards the curing of epoxy with an aim of determining the maximum amount of microballoons that can be dispersed properly within the resin in the absence of a diluent. It has been brought out in the literature that the presence of glass fibers does not affect the curing mechanism, but notable difference in the reaction rates has been observed [39, 40]. We hypothesize that, in view of the physical restraint posed by the glass balloons, the curing process will be adversely affected, especially at high microballoon loadings.

In this article, the rheological profile of glass microballoon filled polymeric syntactic foams using a cycloaliphatic epoxy resin in the presence of two different types of hollow glass microballoons of varying crushing strengths and densities is discussed, to establish the optimal processing conditions.

## 2. Materials and Methods

A low viscosity cycloaliphatic epoxy resin (Ciba Geigy, Araldite CY 230; epoxy equivalent 200 eq  $\text{g}^{-1}$ ,  $\eta \sim 1000$  mPa.s at 30°C ( $\dot{\gamma} = 0.1 \text{ s}^{-1}$ )), a hardener (HY 951; amine content 24 eq  $\text{kg}^{-1}$ ), and hollow glass microballoons (Grades K46 and K15, 3M®) were used without any further treatment. The physical properties of hollow glass microballoons (HGM) used for the preparation of syntactic foams are presented in Table 1.

**2.1. Rheological Studies.** Rheological studies were carried out for HGM-epoxy formulations using an Anton Paar rheometer (MCR 102) using 25 mm disposable aluminum parallel plates. During the experiments, the shear stress was maintained at 1000 Pa to produce reliable and reproducible results. Shear rate sensitivity studies were performed, while varying the shear rate over the range of 0.1 to 1  $\text{s}^{-1}$  under isothermal conditions (30°C). The oscillatory shear flow studies were conducted under both isothermal and dynamic conditions. The test fixture was initially preheated to the

desired temperature. The plates were subsequently separated and the HGM-resin formulation was rapidly inserted. The plates were then brought back to a gap of approximately 1.0 mm and excess sample was trimmed. The experiment was finally initiated when the desired set temperature was achieved. The viscoelastic properties of the sample during cure, including the complex dynamic viscosity ( $\eta^*$ ), shear storage modulus ( $G'$ ), and shear loss modulus ( $G''$ ), were monitored. Experiments were performed over temperatures ranging from 60°C to 100°C in increments of 20°C and temperature sweeps from 30°C to 150°C at a heating rate of 5°C/min were performed using a constant frequency of 1 Hz for all experiments.

**2.2. Processing of Syntactic Foams.** Epoxy based syntactic foams were prepared as per the procedure reported in the literature [10]. The processing steps are as follows: firstly, precalculated amounts of epoxy and hardener (mix ratio of 100:13 by weight) are weighed and mixed together in a suitable beaker for about 5 min. Then, the precalculated amount of microballoon (0–70 vol %) is added while mixing the constituents together by stirring, using a wooden hand spatula (Supplementary Section S1, Table S1). To prevent breakage of hollow microballoons, slow stirring was performed for the uniform dispersion of microspheres. Moreover, due to the low density of the microballoons in comparison to the epoxy resin, the former has a tendency to drift towards the surface of the mold during the curing process. To circumvent the same, the stirring time was adjusted depending upon the amount of microballoon added, to achieve an optimal increase in the viscosity of the mixture. The formulation was degassed and was transferred into silicone molds and placed at 65°C inside an oven for 24 h. Finally, test samples are machined from the cured panel for mechanical and thermal characterization. The nomenclature for the sample is SFxx-yy, where SF refers to syntactic foams, xx denotes the type of glass microballoon employed for processing, i.e., 15 for K15 and 46 for K46, and yy corresponds to the volume percentage of glass microballoons.

**2.3. Quasi-Static Testing.** Mechanical testing was performed on syntactic foams containing 10–70% (v/v) of hollow glass microballoons (K15 and K46) using the Universal Testing Machine (International Equipments). The sample compositions that underwent testing are detailed in the supplementary section, Table S1. For compression, standard specimens of 12 mm diameter and 6 mm thickness were compressed at a crosshead speed of 1.3  $\text{mm min}^{-1}$ . Five specimens of each composition were tested and compressive strength was

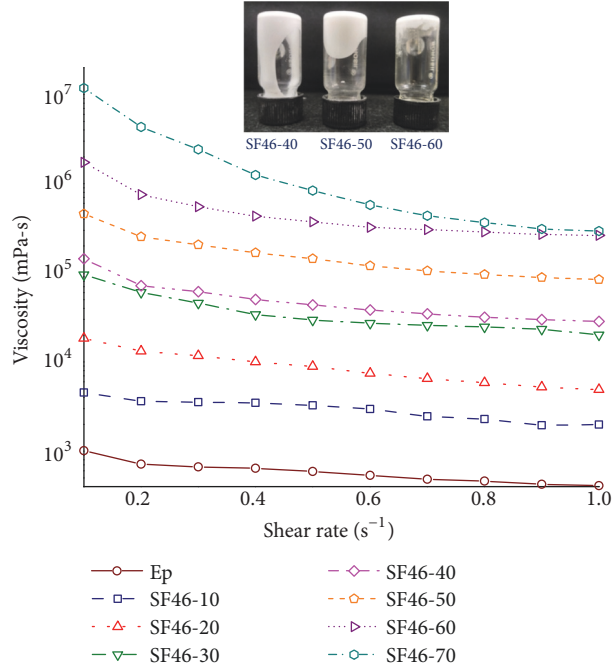


FIGURE 1: Dependence of increasing shear rate and microballoon loading ( $\phi$ ) on viscosity. Inset shows flowability of formulations at 40-60% (v/v) loadings of glass microballoons.

determined from the load-displacement data obtained from the tests. The area under the compressive stress-strain curve till the end of plateau region was quantified to determine the amount of energy absorbed by the foams [41]:

$$E_a = \frac{1}{2} (\sigma_c \times \varepsilon_{crush}) + (\sigma_c \times \varepsilon_{crush}), \quad (1)$$

where  $E_a$ ,  $\sigma_c$ , and  $\varepsilon_{crush}$  refer to the energy absorbed, compressive yield strength, and crushing strain of the foam, respectively.

Flexural testing of syntactic foam specimens of standard dimensions (127 mm length  $\times$  12.5 mm width  $\times$  3.5 mm thickness) was performed by subjecting them to a deformation rate of 2 mm  $\text{min}^{-1}$  and span length of 60 mm under a three-point bending mode as per ASTM D790. The tensile properties were determined as per ASTM D638 using a Universal Testing System (International Equipments) at ambient temperature. The dog bone shaped specimens used for tensile testing were 165 mm long, 3 mm thick, and 13 mm wide along the center of the casting for syntactic foams. The samples were subjected to a crosshead speed of 10 mm  $\text{min}^{-1}$ .

**2.4. Density Determination.** Syntactic foams are usually three phase systems consisting of voids, microballoons, and resin. The presence of voids accounts for a reduction in the experimental density of the syntactic foams [42]. Theoretical density of syntactic foam ( $\rho_{th}$ ) was estimated as per the standard rule of mixtures:

$$\rho_{th} = \rho_{HGM} * \Phi_{HGM} + \rho_{matrix} * \Phi_{matrix}. \quad (2)$$

Experimental density was determined by averaging the mass: volume ratio of five specimens as per ASTM D1622-98. The

ratio of the difference between theoretical and experimental densities to the theoretical density was used to quantify the air void porosity trapped in the matrix during fabrication according to the following equation:

$$\text{Void volume \%} = \frac{\rho_{th} - \rho_{ex}}{\rho_{th}} \times 100. \quad (3)$$

The thermal degradation behavior was investigated using Perkin Elmer Diamond STG-DTA under  $\text{N}_2$  atmosphere in the temperature range 50-600°C. A heating rate of 15°C/min and sample mass of 5.0  $\pm$  0.5 mg were used for each experiment. Calorimetric studies were performed on a differential scanning calorimeter (DSC) (TA Instruments Q20). For dynamic DSC scans, samples (10 $\pm$ 2 mg) were sealed in aluminum pans and heated from 0 to 200°C at 5°C/min. The experiments were performed under flowing  $\text{N}_2$  (50 mL/min) to minimize oxidative degradation of the sample during the curing process. Visual inspection of the hollow glass microballoons was performed using an optical microscope (Olympus) at 40x magnification.

### 3. Results and Discussion

The chemorheological behavior of cycloaliphatic epoxy containing different types of hollow glass microballoons is studied to arrive at the optimal conditions required for processing of syntactic foam formulations.

**3.1. Effect of Microballoon Loading on Viscosity.** The effect of increasing microballoon loading (K46) on the viscosity of the composition in terms of viscosity-shear rate dependence is presented in Figure 1. Compositions prepared using lighter

microballoons (K15) also exhibit a similar profile. It can be seen that the cycloaliphatic epoxy resin exhibits a viscosity of  $\sim 1000$  mPa.s at  $30^\circ\text{C}$  ( $\dot{\gamma}=0.1\text{ s}^{-1}$ ) and the inclusion of microballoons leads to a considerable increase in its viscosity, the extent of which is proportional to the microballoon loading. The data associated with an increase in viscosity as a function of microballoon loading and shear rate is presented in the supplementary section (Figure S1). It is to be noted that, at microballoon loadings  $\sim 60\%$ , the viscosity of the formulation is too high to permit solventless processing. For the sake of visualization, photographs of the representative formulation ( $\phi=40\text{-}60\%$ ) are also included as an inset in Figure 1. It is clear that, for the present system, a microballoon loading of  $60\%$  v/v is the upper limit of fluidity and formulations with higher loading are too viscous to be processed in the absence of a diluent. Our studies indicate that although a theoretical packing efficiency of  $74\%$  is achievable for hexagonal close packing, it is only practical to process foam formulations with HGM loadings  $40\text{-}60\%$  v/v, where the packing of microballoons is random (upper limit =  $64\%$  v/v).

It is to be noted that, in view of the substantial difference in the density of HGM and epoxy, the lighter microballoons tend to drift to the surface of the resin, the time for drifting depending on the density difference. Digital photographs of representative formulations containing varying microballoon (K46) loadings are presented in the supplementary section (Figure S2). At loadings less than or equal to  $30\%$  v/v, separation of the components into distinct layers is evident, with the formation of an upper layer of light, hollow microballoons with epoxy layer at the bottom.

Our study clearly highlights that the curing temperature of epoxy-HGM formulations should be astutely chosen such that the rate of network formation is rapid enough to prevent microballoon agglomeration to the top. The DSC traces associated with the curing of epoxy at different isothermal temperatures are presented in Figure 2. The time associated with the curing process decreases from  $200$  min to  $20$  min as the temperature is raised from  $40$  to  $70^\circ\text{C}$ . For the present scenario, a temperature of  $65^\circ\text{C}$  appears to be appropriate.

Rheological studies can generate valuable inputs with regard to the viscoelastic nature of the material. The rheological profile associated with the curing of microballoon filled compositions was studied under an oscillatory mode using a parallel plate geometry which is routinely used for studying epoxy based systems [43]. The variation in the viscosity for both unfilled and glass microballoon filled compositions ( $40\text{-}60\%$  microballoon loading) is presented in Figure 3. Three distinct regions are clearly evidenced. Initially, a slight decrease in viscosity is observed as the temperature was increased to  $\sim 90^\circ\text{C}$ , which could be attributed to the overcoming of intermolecular interactions with increasing temperature. Further increase in temperature ( $90\text{-}120^\circ\text{C}$ ) leads to a sudden and exponential increase in viscosity: a feature attributable to the autocatalytic nature of curing. As the temperature approaches  $120^\circ\text{C}$ , the viscosity levels off indicating complete curing of the system.

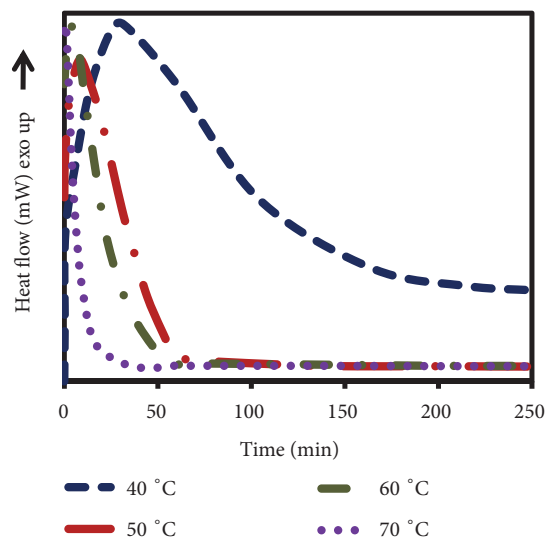


FIGURE 2: Calorimetric traces associated with curing of epoxy at different isothermal temperatures.

The evolution of storage and loss modulus due to curing of representative formulations ( $\phi=40\%$ ) was studied under isothermal temperatures ( $60\text{-}100^\circ\text{C}$ ) to arrive at the optimal temperature required for processing, and the results are presented in Figure 4. The loss modulus is initially higher than the storage modulus because the reactants are in a liquid state. Due to the reaction of the epoxy with amine, both  $G'$  and  $G''$  increase swiftly and a gelation region is observed denoted by crossover of storage and loss modulus. This region marks a sudden transition of the viscous liquid to an elastic solid, where the material can store and dissipate an equal amount of energy and the time required for this is referred to as gelation time ( $t_{\text{gel}}$ ).

Interestingly, when the curing was performed at  $T=60^\circ\text{C}$ , after the initial increase in storage modulus, a slight decrease (in the form of a kink) was observed in the microballoon filled formulations (Figure 4(a)), irrespective of the type of microballoon employed. At lower temperatures, the curing process requires much longer time periods, which reflects in terms of longer " $t_{\text{gel}}$ ." Spherical microballoons tend to roll due to shearing action offered by the plates, and the polymeric network formed is not strong enough to withstand the shearing force offered by the oscillating plates, thereby resulting in its disruption. The network subsequently evolves with time, and the complete curing mandates  $\sim 1$  h. When the curing is performed at higher temperatures (isothermal temperature =  $80\text{-}100^\circ\text{C}$ ), the rate of emergence of the cross-linked structure is much more rapid; therefore the shear force offered by the plates is insufficient to result in any disruption of the network. Although storage and loss modulus are not design parameters, these data can be used to accurately predict the elastic modulus of syntactic foams which will be helpful in engineering applications of such foams [44, 45].

The delay in the curing phenomenon due to inclusion of microballoons in the resin is also evident from the calorimetric studies performed on formulations. Representative

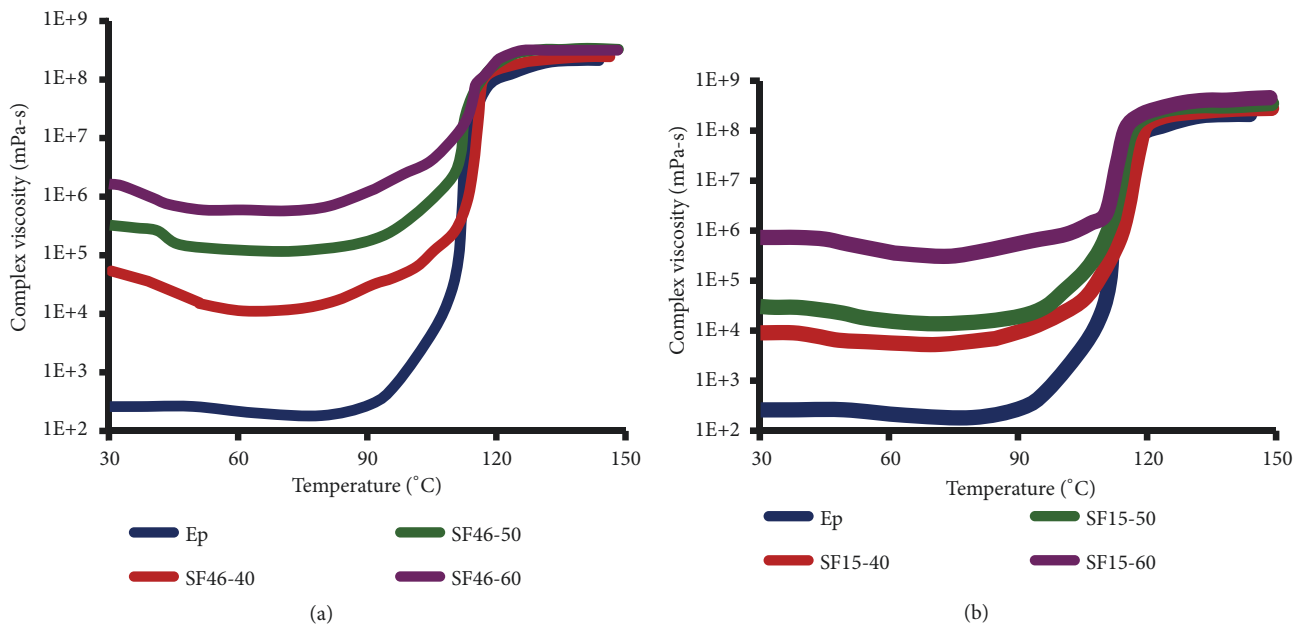


FIGURE 3: The effect of increasing microballoon loading on complex viscosity: (a) K46-epoxy formulations and (b) K15-epoxy formulations.

nonisothermal DSC traces (heating rate=  $10^{\circ}\text{C min}^{-1}$ ) are presented in Figure 5. It can be seen that neat epoxy cures at  $89^{\circ}\text{C}$  ( $T_{\text{peak}}$ ), which is relatively lesser than the  $T_{\text{peak}}$  value associated with formulations containing microballoons.

Gelation time-temperature dependence was used to arrive at the activation energy ( $E_a$ ) associated with the curing process of epoxy, and the results are presented in Figure 6. The detailed procedure for the calculation of  $E_a$  is presented in the supplementary section (Section S2). A substantial delay in curing (as evidenced in terms of longer gelation time) is clear in formulations containing microballoons, a phenomenon attributable to the physical hindrance posed by the microballoons.

The presence of K15 results in a larger delay, which in turn can be attributed to the difference in the thermal conductivity of the microballoons ( $0.05 \text{ Wm}^{-1}\text{K}^{-1}$  for K15 and  $0.15 \text{ Wm}^{-1}\text{K}^{-1}$  for K46), which leads to difference in the heat flow into the epoxy resin [46]. In addition, the role of the difference in the dimensions of the constituent fillers (K15: diameter  $43 \mu\text{m}$ ) as compared to K46 (diameter:  $40 \mu\text{m}$ ) cannot be ruled out.

Interestingly, the activation energy was found to be of the same order in all the formulations, which indicates that the presence of microballoons does not alter the epoxy-amine curing mechanism, which is a classical nucleophilic substitution reaction, reportedly following second-order kinetics [47] (Scheme 1). Our studies are in line with previous studies on glass fiber-epoxy compositions, which revealed that the glass fibers decrease the reaction rate associated with the curing process, without altering the mechanism [39].

**3.2. Voidage in Syntactic Foam.** The theoretical and experimental densities associated with syntactic foams ( $\phi=10\text{-}70\%$ ) are presented in Figure 7. Owing to the higher density of K46

compared to K15 microballoons, cellular samples containing the former microballoons ( $\rho=460 \text{ kg/m}^3$ ) exhibit relatively higher densities than samples containing K15 ( $\rho=150 \text{ kg/m}^3$ ), under similar loadings. The experimental density, however, was much lower than the theoretical values. The difference in the densities was used to evaluate the voidage, which too is included in the figure, the noticeable feature being the higher voidage content in specimens containing high microballoon loading ( $\phi=70\%$ ).

**3.3. Mechanical Properties.** The low density of syntactic foam is the most favorable feature of cellular materials; hence the trends in mechanical properties need to be analyzed with respect to their density, which is best described in terms of specific mechanical properties. The quasi-static properties of the syntactic foams containing varying loadings (10-70% v/v) and different types of microballoons (K15 and K46) are presented in Figure 8. The difference in the crushing strength of the constituent microballoons clearly reflects in the mechanical properties of syntactic foams. The compressive stress-strain curves of epoxy-microballoon syntactic foams at different microballoon volume fractions are presented in the supplementary section (Figure S3). The stress-strain profiles reveal an initial linear elastic (Hookean) region, followed by an energy absorbing plateau region. The peak stress value is the compressive strength of the sample and the plateau region is visualized by an increase in strain without an appreciable increase in stress. In this plateau region, the microballoons are subjected to extensive compressive loads, which results in their crushing. Beyond this, there is an exponential increase in stress without any appreciable increase in strain: a region signaling the onset of densification [8].

Five specimens of each composition were subjected to mechanical tests. All, quasi-static mechanical properties

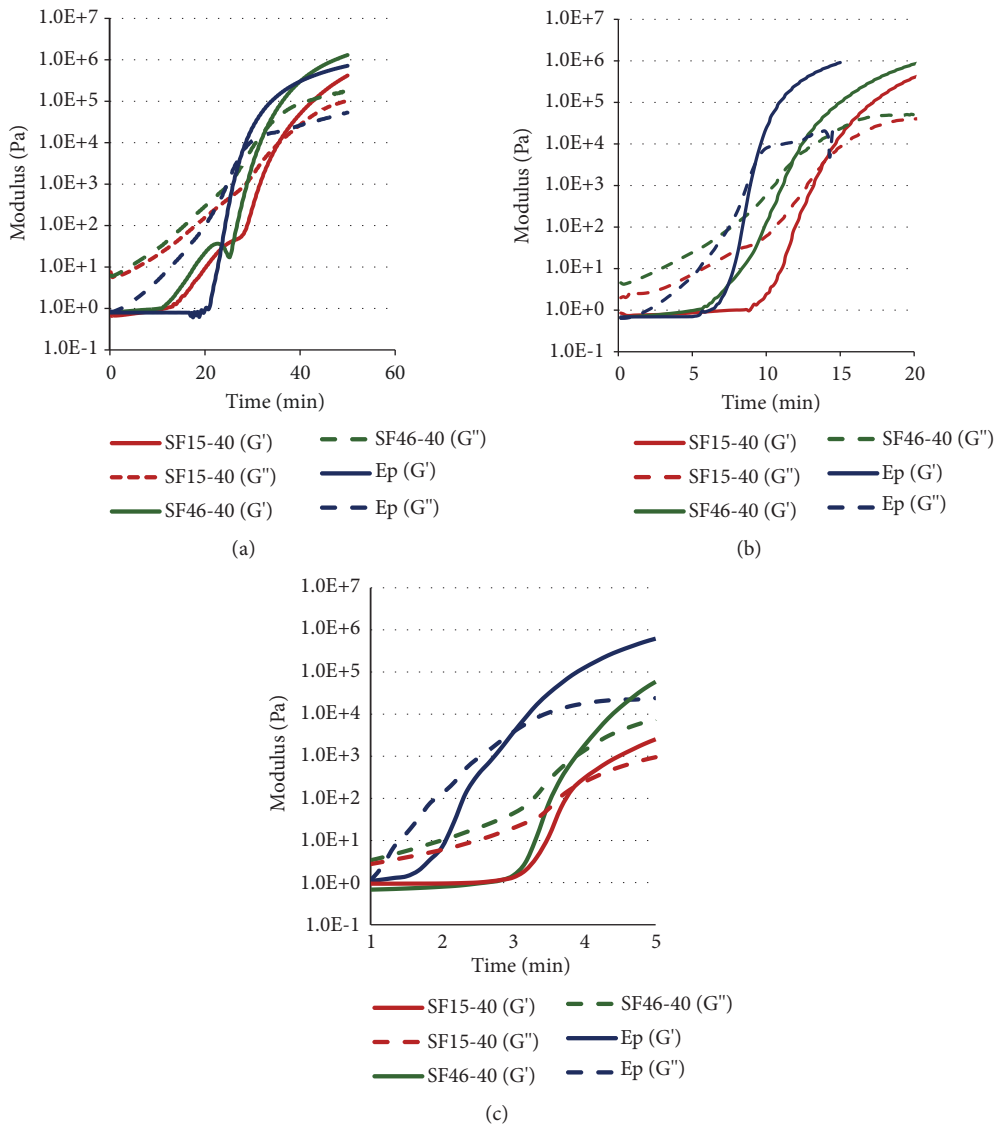


FIGURE 4: Isothermal gelation profiles of resin and syntactic foam formulations at different temperatures: (a) 60°C, (b) 80°C, and (c) 100°C (dotted lines G'', solid lines G').

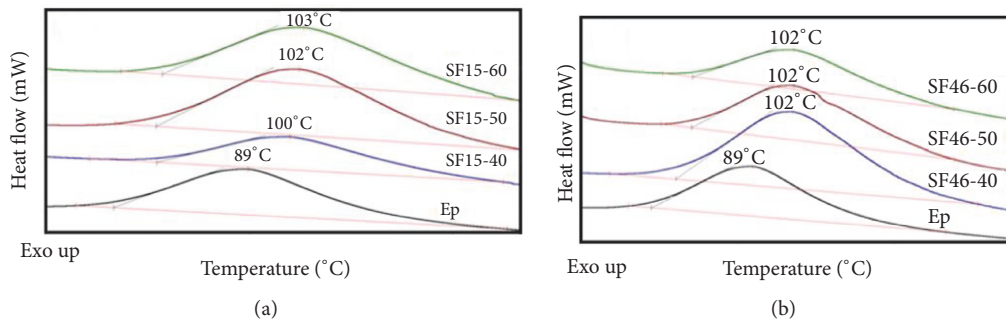


FIGURE 5: Nonisothermal DSC traces for epoxy-HGM formulations with increasing glass microballoons loadings: (a) SF15 and (b) SF46.

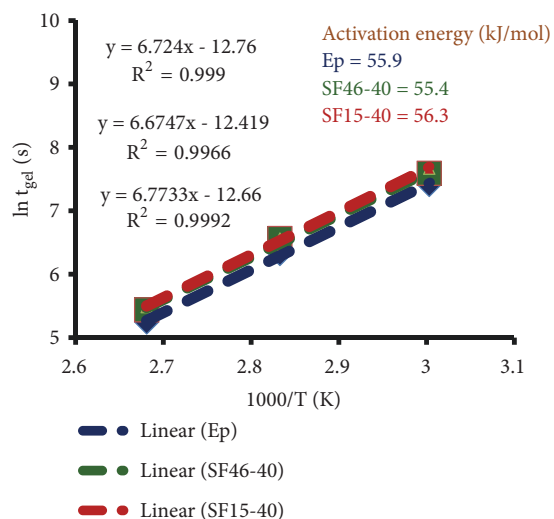


FIGURE 6: Arrhenius plot of  $\ln(t_{gel})$  versus  $1/temperature$ .

irrespective of the testing mode (compressive, tensile, and flexure) were found to decrease with increasing microballoon loading. Microballoon crushing is the primary mechanism responsible for the energy absorption of the foams in the compressive mode [48], which is usually quantified in terms of the area under the stress-strain curve till the end of the plateau region. Under flexural and tensile loadings, the difference between the strengths of two types of a syntactic foam specimen discernibly reduces. It is to be noted that, under the flexure and tensile mode, the microballoons are not the primary load bearing phase and failure depends to a large extent upon the matrix failure [18, 49]. The highest energy absorption ability was exhibited by syntactic foam compositions containing 40% microballoon loading.

What is particularly interesting to note is that the mechanical properties of the cellular materials drop significantly as the microballoon loading is increased to 70% v/v. It is to be noted that the properties of any reinforced material are decided by the extent of interfacial adhesion between the filler and the matrix. A condensation reaction between the surface hydroxyl groups of silica and oxirane rings of epoxy resin is responsible for the excellent adhesion between the glass and epoxy (Scheme S1). The inferior mechanical properties can be attributed to the fact that, in the specimens containing high microballoon loading ( $\sim 70\%$ ), the resin is unable to penetrate into the interstitial regions and inclusion of a large volume percentage of glass microballoons which reportedly exhibit poor crushing strength compared to epoxy. This, in turn, is expected to lead to high voidage, which has also been observed experimentally (Figure 7). The decrease in mechanical properties exceeds the lowering in density; therefore the specific properties are also substantially reduced.

It appears that it is impossible to obtain a hexagonal close-packed structure in syntactic foams using common stir-casting techniques. In common words, packing is defined as a collection of nonoverlapping solid objects in  $n$ -dimensional space. An important attribute of packing is its density  $\phi$ ,

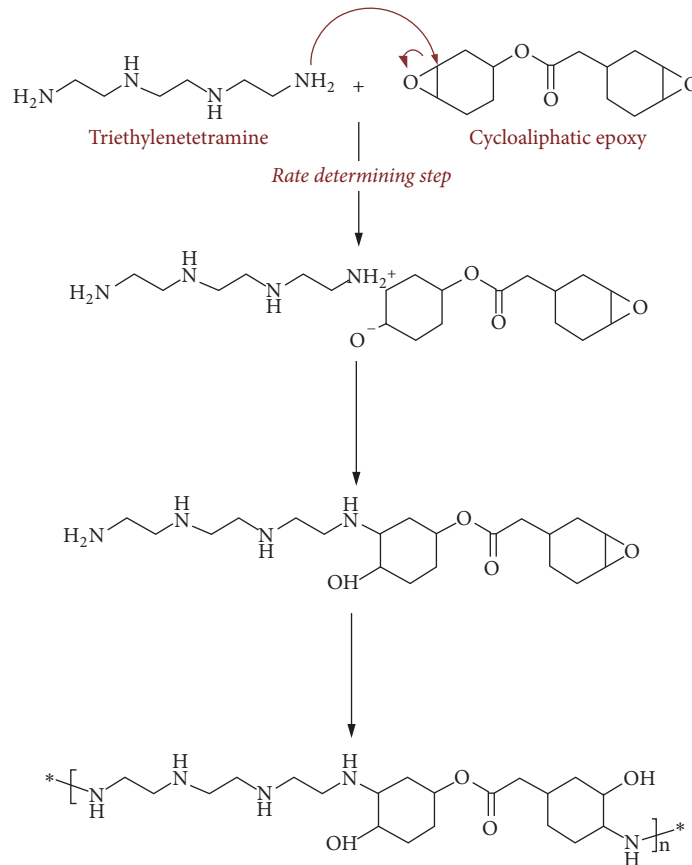
which is defined as the fraction of space covered by the particles. Previously, computer algorithms have been used to study idealized random packing associated with monodisperse spheres. A rate-dependent densification algorithm [24] has indicated that a packing fraction between 0.642 and 0.649 is common. A Monte Carlo scheme yields  $\phi = 0.68$ , while a “drop and roll” algorithm yields a maximal packing efficiency ( $\phi$ ) of 0.60 [25]. Subsequently, a concept of a “Maximally Random Jammed” (MRJ) state was developed, which can be viewed as prototypical glasses in that they are maximally disordered while simultaneously being mechanically rigid. This is associated with a maximum limit of  $\phi = 0.64$  [26]. A pictorial representation of hexagonal packing and random packing is presented in the supplementary section (Figure S4). Our studies indicate that, under the ordinary processing conditions, the “jammed” state appears to be the upper limit of packing with a packing efficiency of 64% [50].

**3.4. Thermal Degradation.** TG-DTG traces of syntactic foams containing K46 microballoons are presented in Figure 9. The thermogravimetric traces of neat epoxy and syntactic foams demonstrated similar profiles barring the progressive increase in the char content from 15.7% to 53% (at 600°C) with increasing microballoons content (10-70% (SF46)). The thermal properties of foams containing K15 present a similar trend and are included in the figure (Figure 9(b)).

Processing of epoxy-glass balloon formulations (40-60% microballoon loading) did not lead to any rupture of glass microballoons under the experimental conditions employed. This was determined by performing oxidative degradation of epoxy syntactic foam specimens in a muffle furnace (at 600°C), and the leftover char was observed under an optical microscope. Representative images of the char obtained from SF46-60 and SF15-60 are presented in Figure 10. It is clear that all the microballoons retained their physical appearance with no evidence of glass rupture.

## 4. Conclusions

In this paper, the rheological behavior associated with the curing of cycloaliphatic epoxy resin in the presence of hollow glass microballoons has been studied to establish optimal conditions for processing. For all practical purposes, compositions with microballoon loading  $< 60\%$  can be conveniently processed using common techniques like stir casting. Formulations with high microballoon loading ( $\geq 60\%$  v/v) exhibit too high viscosities to permit solventless processing of these compositions. This is substantially lower than the theoretical limit of 74% associated with hexagonal close packing. Under ordinary processing conditions, a “random jammed” state appears to be the upper limit of packing, with a packing efficiency of 64%. The presence of microballoons does not alter the epoxy-amine mechanism but the rate of reaction is adversely affected. In view of the density variation between the epoxy and hollow microballoons, the latter tend to drift to the surface. Hence, the curing temperature should be so chosen such that the rate of network formation exceeds the rate of microballoon drifting. In view of the same, a processing temperature of 65°C was found to be



SCHEME 1: Cycloaliphatic epoxy-amine curing reaction mechanism.

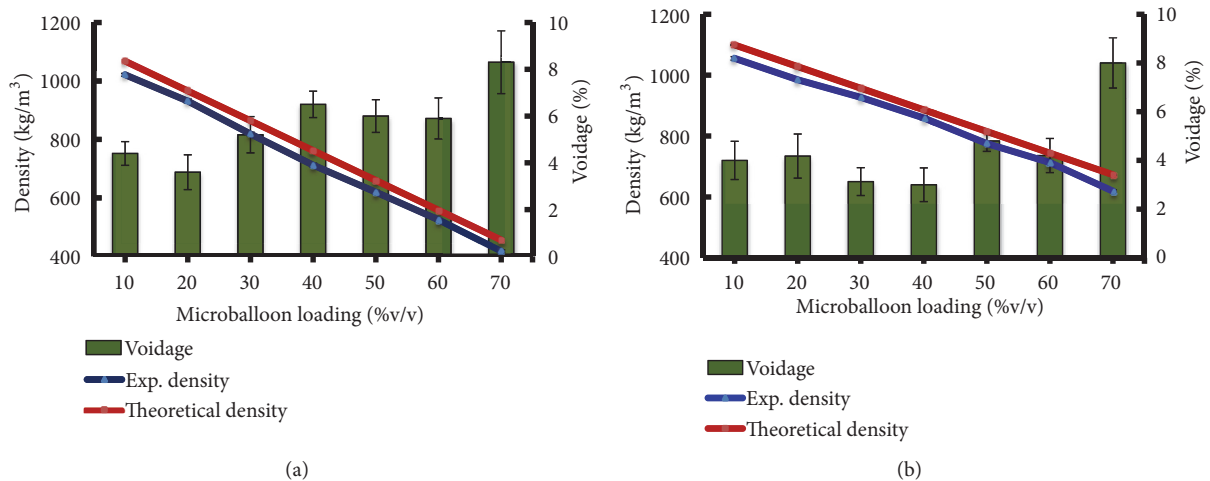


FIGURE 7: Theoretical and experimental densities of syntactic foam specimens: (a) SF15 and (b) SF46. The voidage is presented in the secondary axis.

most appropriate. Mechanical characterization reveals that the quasi-static properties associated with syntactic foams are higher in compositions containing microballoons with higher crushing strength. A concomitant decrease in the quasi-static properties is observed on increasing loadings of either type of glass microballoons; however the mechanical

properties decrease precipitously as the microballoon loading is increased to 70%. An increase of approximately 72% and 192% is observed in the specific toughness values of SF15-40 and SF46-40 syntactic foams, respectively, compared to neat epoxy. The microballoons did not undergo any significant rupture under the conditions employed during processing.



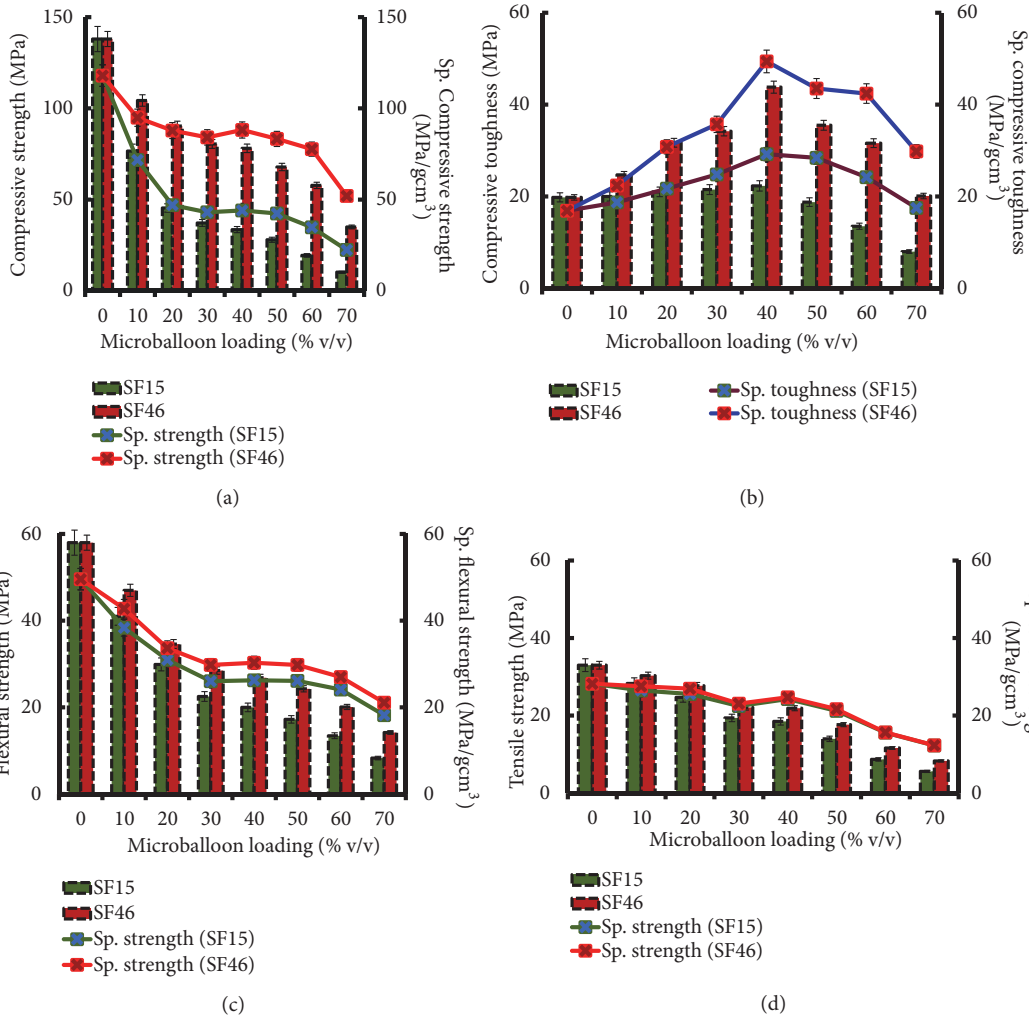


FIGURE 8: (a-b) Compressive, (c) flexural, and (d) tensile properties of epoxy syntactic foams containing different microballoons at varying loadings.

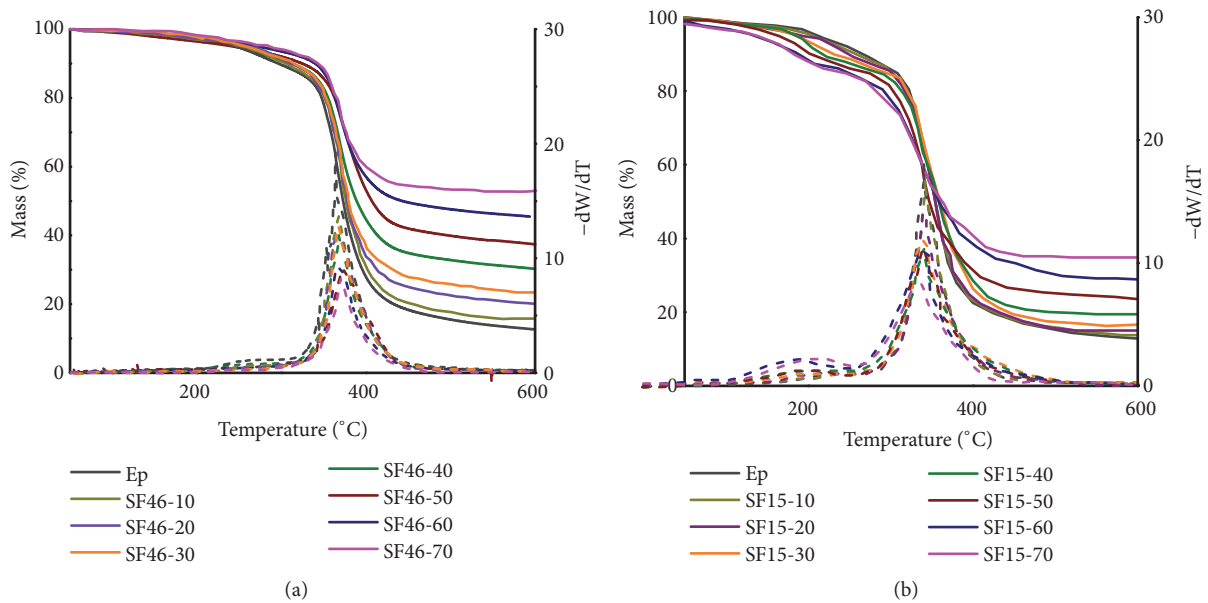


FIGURE 9: TG-DTG traces of epoxy syntactic foams: (a) SF46 and (b) SF15 (dotted lines represent DTG).

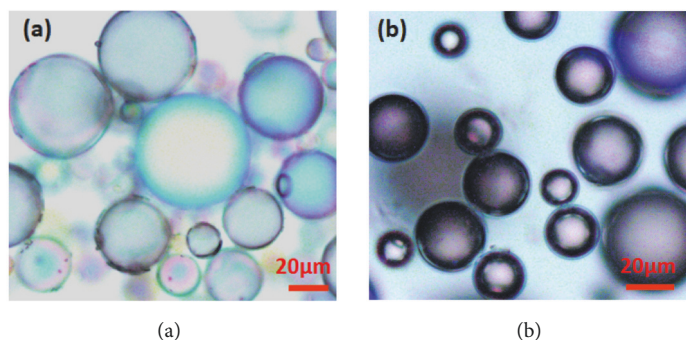


FIGURE 10: Optical images of the char obtained after oxidative degradation of (a) SF15-60 and (b) SF46-60.

## Data Availability

The data used to support the findings of this study are included in the manuscript and supplementary material.

## Conflicts of Interest

The authors declare that there are no conflicts of interest regarding the publication of this paper.

## Acknowledgments

The authors would like to thank DRDO for funding this work through ST/14-15/CFE-1311. A. V. Ullas is pleased to acknowledge DTU for providing financial support.

## Supplementary Materials

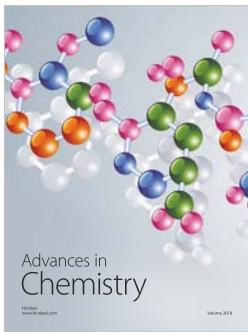
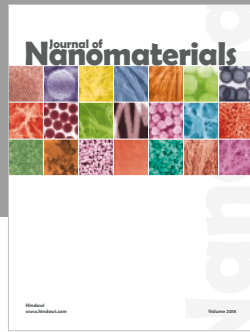
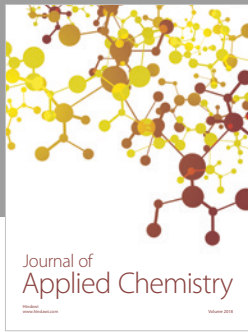
Section S1: calculation of the amount of hollow glass microballoons. Table S1: compositional details of syntactic foam. Figure S1: increase in viscosity as a function of microballoon loading and shear rate ( $\dot{\gamma}$ ). Figure S2: drifting of microballoons to the surface of epoxy-HGM formulations with varying glass microballoon loadings: (a) 10, (b) 20, (c) 30, and (d) 40% (v/v). Section S2: activation energy calculation. Table S2: variation of gelation time ( $t_{gel}$ ) with temperature (T) and activation energy for syntactic foam compositions. Figure S3: representative compressive stress-strain curves of (a) SF15 and (b) SF46 syntactic foams. Figure S4: close packing in syntactic foams: (a) random packing (packing efficiency  $\sim 64\%$ ) and (b) hexagonal close packing (packing efficiency  $\sim 74\%$ ). Scheme S1: reaction of hydroxyl groups in glass with epoxy. (*Supplementary Materials*)

## References

- [1] D. Pinisetty, V. C. Shunmugasamy, and N. Gupta, *6 - Hollow Glass Microspheres in Thermosets—Epoxy Syntactic Foams*, William Andrew Publishing: Oxford, UK, 2015.
- [2] A. Ullas, D. Kumar, and P. K. Roy, “Poly(dimethylsiloxane)-toughened syntactic foams,” *Journal of Applied Polymer Science*, vol. 135, no. 8, p. 45882, 2018.
- [3] H. Mae, M. Omiya, and K. Kishimoto, “Effects of strain rate and density on tensile behavior of polypropylene syntactic foam with polymer microballoons,” *Materials Science and Engineering: A Structural Materials: Properties, Microstructure and Processing*, vol. 477, no. 1-2, pp. 168–178, 2008.
- [4] N. Jha, D. P. Mondal, M. D. Goel, J. D. Majumdar, S. Das, and O. P. Modi, “Titanium cenosphere syntactic foam with coarser cenosphere fabricated by powder metallurgy at lower compaction load,” *Transactions of Nonferrous Metals Society of China*, vol. 24, no. 1, pp. 89–99, 2014.
- [5] R. L. Poveda and N. Gupta, “Carbon-nanofiber-reinforced syntactic foams: compressive properties and strain rate sensitivity,” *JOM: The Journal of The Minerals, Metals & Materials Society (TMS)*, vol. 66, no. 1, pp. 66–77, 2013.
- [6] D. Benderly, Y. Rezek, J. Zafran, and D. Gorni, “Effect of composition on the fracture toughness and flexural strength of syntactic foams,” *Polymer Composites*, vol. 25, no. 2, pp. 229–236, 2004.
- [7] M. Colloca, N. Gupta, and M. Porfiri, “Tensile properties of carbon nanofiber reinforced multiscale syntactic foams,” *Composites Part B: Engineering*, vol. 44, no. 1, pp. 584–591, 2013.
- [8] N. Gupta, Kishore, E. Woldesenbet, and S. Sankaran, “Studies on compressive failure features in syntactic foam material,” *Journal of Materials Science*, vol. 36, no. 18, pp. 4485–4491, 2001.
- [9] A. V. Ullas, P. K. Shaima, P. Chandel et al., “Epoxy-glass microballoon syntactic foams for blast mitigating application,” *Defence Science Journal*, vol. 68, no. 2, pp. 210–217, 2018.
- [10] A. V. Ullas, B. Qayyum, D. Kumar, and P. K. Roy, “Electrospun polyamide nanofiber-reinforced hybrid syntactic foams,” *Polymer—Plastics Technology and Engineering*, vol. 55, no. 17, pp. 1797–1806, 2016.
- [11] A. Pellegrino, V. L. Tagarielli, R. Gerlach, and N. Petrinic, “The mechanical response of a syntactic polyurethane foam at low and high rates of strain,” *International Journal of Impact Engineering*, vol. 75, pp. 214–221, 2015.
- [12] L. Bardella, F. Malanca, P. Ponzio, A. Panteghini, and M. Porfiri, “A micromechanical model for quasi-brittle compressive failure of glass-microballoons/thermoset-matrix syntactic foams,” *Journal of the European Ceramic Society*, vol. 34, no. 11, pp. 2605–2616, 2014.
- [13] A. Panteghini and L. Bardella, “On the compressive strength of glass microballoons-based syntactic foams,” *Mechanics of Materials*, vol. 82, pp. 63–77, 2015.
- [14] K. A. Devi, B. John, C. P. R. Nair, and K. N. Ninan, “Syntactic foam composites of epoxy-allyl phenol-bismaleimide ternary blend - processing and properties,” *Journal of Applied Polymer Science*, vol. 105, no. 6, pp. 3715–3722, 2007.

- [15] J. R. M. D'Almeida, "An analysis of the effect of the diameters of glass microspheres on the mechanical behavior of glass-microsphere/epoxy-matrix composites," *Composites Science and Technology*, vol. 59, no. 14, pp. 2087–2091, 1999.
- [16] R. Huang and P. Li, "Elastic behaviour and failure mechanism in epoxy syntactic foams: The effect of glass microballoon volume fractions," *Composites Part B: Engineering*, vol. 78, pp. 401–408, 2015.
- [17] C. S. Karthikeyan, S. Sankaran, and Kishore, "Elastic behaviour of plain and fibre-reinforced syntactic foams under compression," *Materials Letters*, vol. 58, no. 6, pp. 995–999, 2004.
- [18] L. Wang, J. Zhang, X. Yang, C. Zhang, W. Gong, and J. Yu, "Flexural properties of epoxy syntactic foams reinforced by fiberglass mesh and/or short glass fiber," *Materials and Corrosion*, vol. 55, pp. 929–936, 2014.
- [19] M. V. Alonso, M. L. Auad, and S. Nutt, "Short-fiber-reinforced epoxy foams," *Composites Part A: Applied Science and Manufacturing*, vol. 37, no. 11, pp. 1952–1960, 2006.
- [20] T. C. Lin, N. Gupta, and A. Talalayev, "Thermoanalytical characterization of epoxy matrix-glass microballoon syntactic foams," *Journal of Materials Science*, vol. 44, no. 6, pp. 1520–1527, 2009.
- [21] S. Kang, S. I. Hong, C. R. Choe, M. Park, S. Rim, and J. Kim, "Preparation and characterization of epoxy composites filled with functionalized nanosilica particles obtained via sol-gel process," *Polymer Journal*, vol. 42, no. 3, pp. 879–887, 2010.
- [22] J. Gassan and A. K. Bledzki, "Possibilities for improving the mechanical properties of jute/epoxy composites by alkali treatment of fibres," *Composites Science and Technology*, vol. 59, no. 9, pp. 1303–1309, 1999.
- [23] K. R. Dando, W. M. Cross, M. J. Robinson, and D. R. Salem, "Production and characterization of epoxy syntactic foams highly loaded with thermoplastic microballoons," *Journal of Cellular Plastics*, vol. 54, no. 3, pp. 499–514, 2018.
- [24] W. S. Jodrey and E. M. Tory, "Computer simulation of close random packing of equal spheres," *Physical Review A: Atomic, Molecular and Optical Physics*, vol. 32, no. 4, pp. 2347–2351, 1985.
- [25] W. M. Visscher and M. Bolsterli, "Random packing of equal and unequal spheres in two and three dimensions," *Nature*, vol. 239, no. 5374, pp. 504–507, 1972.
- [26] S. Torquato, T. M. Truskett, and P. G. Debenedetti, "Is random close packing of spheres well defined?" *Physical Review Letters*, vol. 84, no. 10, pp. 2064–2067, 2000.
- [27] M. C. Saha, S. Nilufar, M. Major, and S. Jeelani, "Processing and performance evaluation of hollow microspheres filled epoxy composites," *Polymer Composites*, vol. 29, no. 3, pp. 293–301, 2008.
- [28] N. Gupta and E. Woldesenbet, "Hygrothermal studies on syntactic foams and compressive strength determination," *Composite Structures*, vol. 61, no. 4, pp. 311–320, 2003.
- [29] R. R. Maharsia and H. D. Jerro, "Enhancing tensile strength and toughness in syntactic foams through nanoclay reinforcement," *Materials Science and Engineering: A Structural Materials: Properties, Microstructure and Processing*, vol. 454–455, pp. 416–422, 2007.
- [30] K. S. Santhosh Kumar, C. P. Reghunadhan Nair, and K. N. Ninan, "Mechanical properties of polybenzoxazine syntactic foams," *Journal of Applied Polymer Science*, vol. 108, no. 2, pp. 1021–1028, 2008.
- [31] F. A. Shutov, "Syntactic polymer foams," in *Chromatography/Foams/Copolymers*, vol. 73/74 of *Advances in Polymer Science*, pp. 63–123, Springer Berlin Heidelberg, Berlin, Germany, 1986.
- [32] P. Bunn and J. T. Mottram, "Manufacture and compression properties of syntactic foams," *Composites Part B: Engineering*, vol. 24, no. 7, pp. 565–571, 1993.
- [33] M. M. Islam and H. S. Kim, "Manufacture of syntactic foams: pre-mold processing," *Materials and Manufacturing Processes*, vol. 22, no. 1, pp. 28–36, 2007.
- [34] P. Pötschke, T. D. Fornes, and D. R. Paul, "Rheological behavior of multiwalled carbon nanotube/polycarbonate composites," *Polymer Journal*, vol. 43, no. 11, pp. 3247–3255, 2002.
- [35] H.-W. Xiao, S.-Q. Huang, and T. Jiang, "Morphology, rheology, and mechanical properties of dynamically cured epdm/pp blend: effect of curing agent dose variation," *Journal of Applied Polymer Science*, vol. 92, no. 1, pp. 357–362, 2004.
- [36] A. K. Jain, N. K. Gupta, and A. K. Nagpal, "Effect of dynamic cross-linking on melt rheological properties of polypropylene/ethylene-propylene-diene rubber blends," *Journal of Applied Polymer Science*, vol. 77, no. 7, pp. 1488–1505, 2000.
- [37] P. J. Halley and M. E. Mackay, "Chemorheology of thermosets—an overview," *Polymer Engineering & Science*, vol. 36, no. 5, pp. 593–609, 1996.
- [38] M. B. Roller, "Rheology of curing thermosets: a review," *Polymer Engineering & Science*, vol. 26, no. 6, pp. 432–440, 1986.
- [39] M.-F. Grenier-Loustalot and P. Grenier, "The mechanism of epoxy-resin curing in the presence of glass and carbon fibres," *Polymer Journal*, vol. 33, no. 6, pp. 1187–1199, 1992.
- [40] V. M. Karbhari and R. Lee, "On the effect of E-glass fiber on the cure behavior of vinyl ester composites," *Journal of Reinforced Plastics and Composites*, vol. 21, no. 11, pp. 901–918, 2002.
- [41] P. Raghu, S. Kunigal, and R. Larry, "Energy absorption performance of a eco-core - a syntactic foam," in *Proceedings of the 48th Aiaa/Asme/Asce/Ahs/Asc Structures, Structural Dynamics, And Materials Conference*, American Institute of Aeronautics and Astronautics, 2007.
- [42] M. Narkis, S. Kenig, and M. Puterman, "Three-phase syntactic foams," *Polymer Composites*, vol. 5, no. 2, pp. 159–165, 1984.
- [43] M. Ivankovic, L. Incarnato, J. M. Kenny, and L. Nicolais, "Curing kinetics and chemorheology of epoxy/anhydride system," *Journal of Applied Polymer Science*, vol. 90, no. 11, pp. 3012–3019, 2003.
- [44] S. E. Zeltmann, K. A. Prakash, M. Doddamani, and N. Gupta, "Prediction of modulus at various strain rates from dynamic mechanical analysis data for polymer matrix composites," *Composites Part B: Engineering*, vol. 120, pp. 27–34, 2017.
- [45] S. E. Zeltmann, B. R. Bharath Kumar, M. Doddamani, and N. Gupta, "Prediction of strain rate sensitivity of high density polyethylene using integral transform of dynamic mechanical analysis data," *Polymer Journal*, vol. 101, pp. 1–6, 2016.
- [46] S. Park, F. Jin, and C. Lee, "Preparation and physical properties of hollow glass microspheres-reinforced epoxy matrix resins," *Materials Science and Engineering: A Structural Materials: Properties, Microstructure and Processing*, vol. 402, no. 1–2, pp. 335–340, 2005.
- [47] J.-E. Ehlers, N. G. Rondan, L. K. Huynh, H. Pham, M. Marks, and T. N. Truong, "Theoretical study on mechanisms of the epoxy-amine curing reaction," *Macromolecules*, vol. 40, no. 12, pp. 4370–4377, 2007.

- [48] M. Dimchev, R. Caeti, and N. Gupta, "Effect of carbon nanofibers on tensile and compressive characteristics of hollow particle filled composites," *Materials and Corrosion*, vol. 31, no. 3, pp. 1332–1337, 2010.
- [49] N. Gupta and R. Nagorny, "Tensile properties of glass microballoon-epoxy resin syntactic foams," *Journal of Applied Polymer Science*, vol. 102, no. 2, pp. 1254–1261, 2006.
- [50] C. Song, P. Wang, and H. A. Makse, "A phase diagram for jammed matter," *Nature*, vol. 453, no. 7195, pp. 629–632, 2008.



**Hindawi**  
Submit your manuscripts at  
[www.hindawi.com](http://www.hindawi.com)

